



Cite this: *Phys. Chem. Chem. Phys.*, 2024, 26, 4840

Received 8th September 2023,
Accepted 2nd January 2024

DOI: 10.1039/d3cp04364a

rsc.li/pccp

For the first time, we directly measured the onset and completion temperatures of polymorphic transitions under thermo-mechanochemical conditions by simultaneous *in situ* synchrotron powder X-ray diffraction and temperature monitoring. We determined the thermo-mechanochemical polymorphic transition temperature in 1-adamantyl-1-diamantyl ether to be 31 °C lower than the transition temperature determined by DSC. Our findings highlight the uniqueness of thermo-mechanochemical conditions, with potential applications in polymorph screening.

Crystal polymorphism is of tremendous importance in pharmaceuticals,¹ dyes,² semiconductors,³ porous materials,⁴ crystal adaptronics,⁵ etc. Ascertaining the thermodynamic relationship between different polymorphs of the same compound is crucial for their application. According to the heat of transition rule, polymorphs are in an enantiotropic relationship if the transition between them occurs below their melting points, which is typically established by differential scanning calorimetry (DSC) experiment.⁶ In the case of a monotropic relationship, there is no interconversion between polymorphs. Experimentally measured transition temperature by DSC mostly does not correspond to the thermodynamic transition temperature. Namely, the hysteresis between the experimental and thermodynamic transition temperature is due to the kinetic barrier, which includes nucleation and phase propagation barriers that may be considerable near the transition point.⁷

^a Ruđer Bošković Institute, Bijenička 54, 10 000 Zagreb, Croatia.
E-mail: jasna.alic@irb.hr, marina.sekutor@irb.hr, krunoslav.uzarevic@irb.hr, tomislav.stolar@gmail.com

^b Deutsches Elektronen-Synchrotron (DESY), Notkestraße 85, 22 607 Hamburg, Germany

^c Department of Chemistry, Faculty of Science, University of Zagreb, Horvatovac 102a, 10 000 Zagreb, Croatia

† Electronic supplementary information (ESI) available. CCDC 2270174. For ESI and crystallographic data in CIF or other electronic format see DOI: <https://doi.org/10.1039/d3cp04364a>

‡ Current address: Federal Institute for Materials Research and Testing (BAM), Richard-Willstätter-Straße 11, 12489 Berlin, Germany.

Direct *in situ* measurement of polymorphic transition temperatures under thermo-mechanochemical conditions†

Jasna Alić, ^a Ivor Lončarić, ^a Martin Etter, ^b Mirta Rubčić, ^c Zoran Štefanić, ^a Marina Šekutor, ^a Krunoslav Užarević ^a and Tomislav Stolar ^a [‡]

Ball milling^{8–10} efficiently introduces crystal defects that lead to polymorphic transitions.¹¹ The polymorphic outcome of mechanochemical reactions is highly sensitive to the reaction conditions in neat grinding (NG), liquid-assisted grinding (LAG),^{12–15} ion and liquid-assisted grinding,¹⁶ and polymer-assisted grinding¹⁷ approaches. It can also be modified by using different milling jars^{18,19} and balls.²⁰ Notably, polymorphic transitions induced by milling can modify the bulk temperature of the reaction mixture.²¹ Recently, Emmerling and Michalchuk have shown how thermo-mechanochemical conditions lowered the polymorphic transition temperature in isonicotinamide and glutaric acid cocrystals by at least 15 °C compared to the corresponding DSC transition temperature.²² These experiments were conducted by heating milling jars to the desired temperature setpoints, after which isothermal ball milling was monitored *in situ* by synchrotron powder X-ray diffraction (PXRD).²² Motivated by that report, we aimed to use ramp heating and directly determine the onset and completion temperatures of polymorphic transitions under thermo-mechanochemical conditions[§] by *in situ* synchrotron PXRD^{23–25} and thermal control of milling (Fig. 1).^{26,27}

Here, we study polymorphism in a diamondoid derivative, 1-adamantyl-1-diamantyl ether (ADE).²⁸ Diamondoids are thermodynamically stable cage hydrocarbons whose scaffolds mimic the arrangement of carbon atoms in a diamond crystal lattice.²⁹ Owing to their unique properties, diamondoid derivatives hold

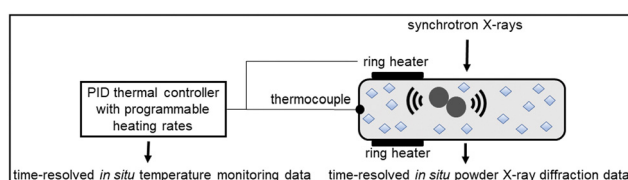


Fig. 1 Our setup for direct measurement of polymorphic transition temperatures under thermo-mechanochemical conditions by simultaneous *in situ* synchrotron powder X-ray diffraction and temperature monitoring.



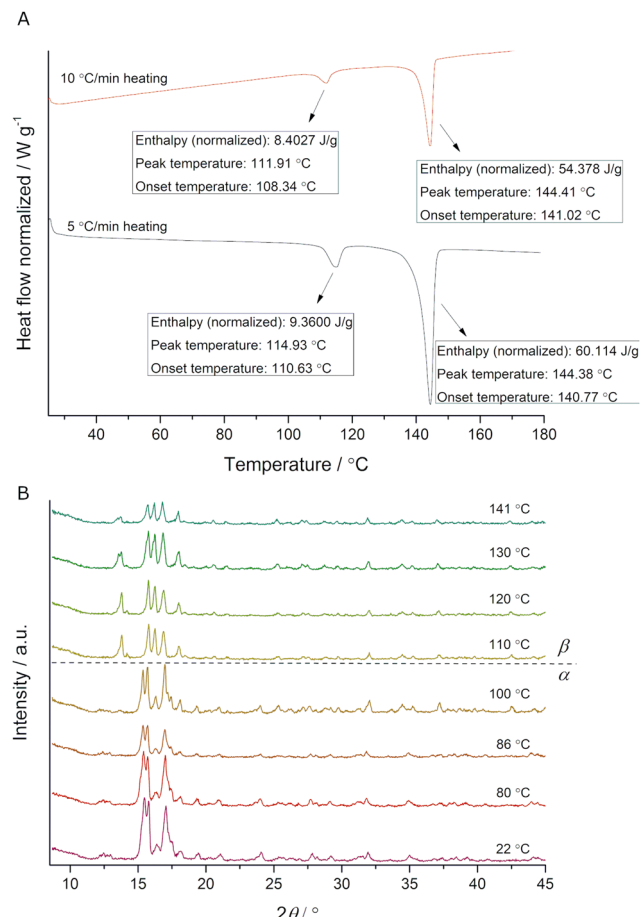


Fig. 2 (A) DSC traces of **ADE** obtained by applying different heating rates. Endotherms are pointing downwards. (B) *In situ* monitoring of **ADE** phase transition by VT-PXRD ($\lambda = 1.54 \text{ \AA}$).

immense potential for application in fields ranging from polymers and surface coatings to organocatalysis, drugs, and molecular electronics.^{29–31} In the solid state, these molecules frequently exhibit phenomena such as order-disorder phase transitions^{32–35} and polymorphism.^{36–39}

While performing DSC analysis of **ADE** prepared by thermo-mechanochemistry,⁴⁰ we observed an endotherm prior to its melting point (Fig. 2A). More specifically, the presence of an endotherm peak around 112 °C (Fig. 2A red), which appeared before melting endotherm at 144 °C, indicated a phase transition. In a repeated DSC experiment, we heated the starting compound to 115 °C, and PXRD analysis showed the appearance of a new crystalline phase (ESI,† Fig. S1). When applying a different heating rate, we established a shift of the signal related to a polymorph transition (Fig. 2A black), an indication of a kinetically irreversible phase transition.⁶ Additionally, *in situ* variable-temperature PXRD (VT-PXRD) measurements showed a phase transition between 100 °C and 110 °C (Fig. 2B), in excellent agreement with DSC results.

Analysis by gas chromatography coupled with mass spectrometry (GC-MS) confirmed the presence of **ADE**, leading us to conclude that we indeed obtained a new polymorph of **ADE**,²⁸

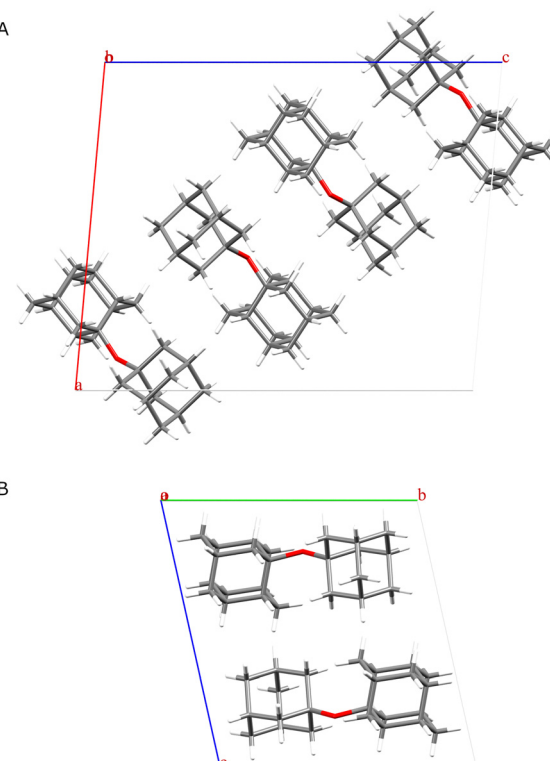


Fig. 3 Depiction of the crystal structure of: (A) polymorph α (shown down the b -axis), (B) polymorph β (shown down the a -axis).

which was further corroborated by ^1H – ^{13}C cross-polarization magic angle spinning nuclear magnetic resonance spectra (CPMAS) (ESI,† Fig. S2). To obtain single crystals for the purpose of structural studies *via* X-ray diffraction, we recrystallised the sample that was heated to 115 °C in several solvents, including diethyl ether, *n*-pentane, and THF (ESI,† Fig. S3). Pleasingly, crystals grown in THF corresponded to the newly discovered form. We solved the crystal structure of the new phase from single-crystal X-ray diffraction data (ESI,† Table S1) and confirmed that **ADE** has at least two polymorphic forms, a room-temperature (RT) form named polymorph α , and a high-temperature form named polymorph β (Fig. 3, ESI,† Fig. S4). Polymorph α crystallises in a monoclinic $P2/n$ space group with four molecules of **ADE** in the unit cell, while polymorph β crystallises in a triclinic $P\bar{1}$ space group with two molecules of **ADE** in the unit cell. As expected for diamondoid ether derivatives, molecules in α and β polymorphs are stabilised *via* London dispersion intermolecular interactions.⁴¹

Next, we explored the possibility of polymorph interconversion under mechanochemical conditions. We performed NG of polymorph α at RT. However, the transition to high-temperature polymorph β did not occur after 1 h of milling at 30 Hz (ESI,† Fig. S5). Moreover, $\alpha \rightarrow \beta$ transition did not occur even after LAG of polymorph α with THF, the same solvent from which single crystals of polymorph β were grown, at RT for 1 h (ESI,† Fig. S5). On the other hand, NG of polymorph β at RT for 24 h resulted in a mixture of polymorphs (ESI,† Fig. S6), consistent with polymorph β being metastable at RT, while the LAG of polymorph β

with *n*-pentane resulted in a full transition to RT polymorph α after 45 min of milling at ambient conditions (ESI,† Fig. S5).

We then turned to thermo-mechanochemical experiments with simultaneous mechanical and thermal activation and monitored them *in situ* by synchrotron PXRD (Fig. 1 and ESI,† Fig. S7 and S8). In the first experiment, we used a ramp heating rate of $2\text{ }^{\circ}\text{C min}^{-1}$ for milling of polymorph α (for details see ESI†). Time-resolved *in situ* PXRD data showed the onset of a polymorphic transition to polymorph β after 30 min of milling (Fig. 4A and B) when the temperature of the milling reactor reached $86\text{ }^{\circ}\text{C}$ (Fig. 4C). Both polymorphs co-existed until the milling temperature reached $90\text{ }^{\circ}\text{C}$, after which only polymorph β was present, thus indicating completion of the $\alpha \rightarrow \beta$ transition. In the second experiment, the obtained polymorph β was milled under LAG conditions with *n*-pentane as a liquid additive at RT. After *ca.* 6 min of milling, we observed a gradual disappearance of the diffraction peaks corresponding to β (ESI,† Fig. S9). However, we attributed this feature to the change in the rheology of the reaction mixture† and the inhomogeneous distribution of the milled sample, which led to its disappearance from the X-ray beam. Nevertheless, the same sample was again milled but this time heated at a faster rate without ramp heating (Fig. 4F). Immediately after the heating started, we observed the appearance of diffraction peaks, which at the temperature of $73\text{ }^{\circ}\text{C}$ were more pronounced and clearly showed the presence of α (Fig. 4D). In continuation of the same experiment, the onset of the $\alpha \rightarrow \beta$ transition was observed at $100\text{ }^{\circ}\text{C}$ after only 4.4 min of milling

and finished after 4.9 min of milling at a milling temperature of $108\text{ }^{\circ}\text{C}$ (Fig. 4D and E). Hence, thermo-mechanochemical experiments with different heating rates demonstrated that both milling temperature and time markedly influence the polymorphic transition temperature.

We next conducted laboratory *ex situ* experiments to complement the *in situ* studies. For example, we repeated the ramp heating experiment (using $2\text{ }^{\circ}\text{C min}^{-1}$ heating rate) of milling polymorph α and stopped the reaction after reaching $87\text{ }^{\circ}\text{C}$. Subsequent *ex situ* PXRD analysis confirmed the presence of both polymorphs in the reaction mixture (ESI,† Fig. S10), thus reproducing the results that we obtained at the synchrotron facility (Fig. 4B). We were also curious to see if we could lower the thermo-mechanochemical transition temperature even further by varying milling temperature and time parameters. Importantly, after isothermal milling of polymorph α at $81\text{ }^{\circ}\text{C}$ for 1 h, pure polymorph β was obtained (ESI,† Fig. S11). However, further lowering of the milling temperature to $71\text{ }^{\circ}\text{C}$ and extension of milling time to 2 h did not result in a polymorphic transition, which was also the case after continuing to mill the same sample for an additional 24 h at $71\text{ }^{\circ}\text{C}$ (ESI,† Fig. S12). We also performed LAG of polymorph α for 2 h at $71\text{ }^{\circ}\text{C}$ with THF as a liquid additive but $\alpha \rightarrow \beta$ transition did not occur (ESI,† Fig. S12). Thus, the lowest detected limit for $\alpha \rightarrow \beta$ transition by thermo-mechanochemistry was $81\text{ }^{\circ}\text{C}$.

So far, we observed a remarkable decrease in the polymorphic transition temperature under thermo-mechanochemical conditions compared to that obtained in DSC. We then turned to

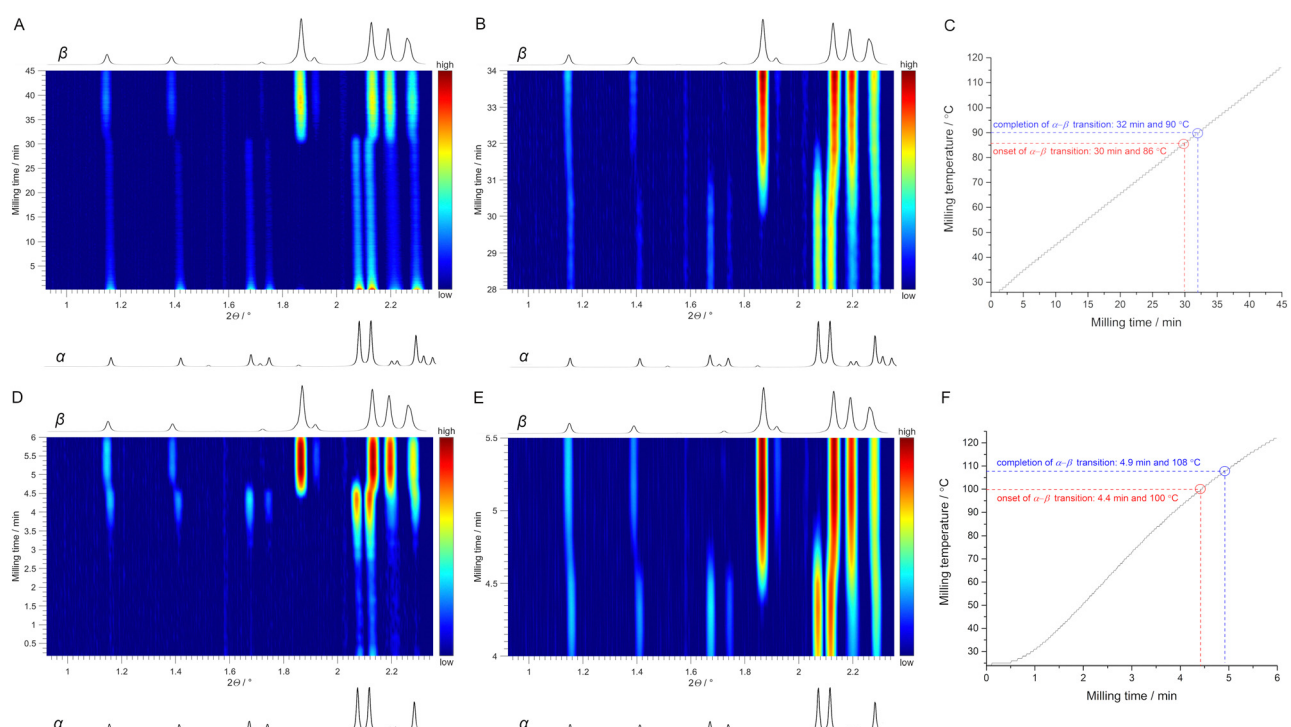


Fig. 4 *In situ* monitoring of milling ADE under different heating regimes by synchrotron PXRD ($\lambda = 0.20741\text{ \AA}$). (A) With ramp heating. (B) Zoomed in region of (A). (C) Plotted data for milling temperatures associated with (A) and (B). (D) Heating without ramp. (E) Zoomed in region of (D). (F) Plotted data for milling temperatures associated with (D) and (E).



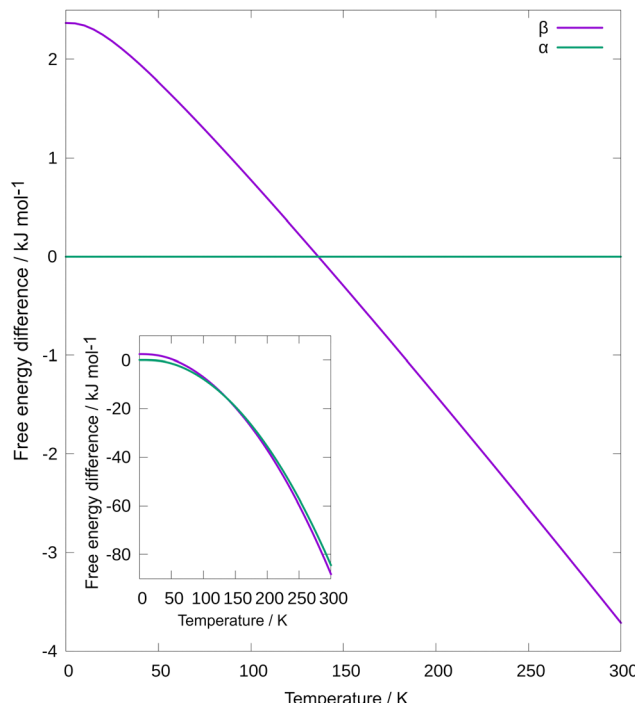


Fig. 5 Difference of Helmholtz free energies $F_\beta - F_\alpha$ as a function of temperature. Inset: Helmholtz free energy as a function of temperature for both polymorphs.

computational tools to get a better understanding of overcoming the kinetic barrier for polymorphic transition through thermo-mechanochemical treatment. As shown in Fig. 5, we have calculated Helmholtz free energy as a function of temperature for both polymorphs.

We calculated internal energy with density functional theory at the PBE⁴² + MBD⁴³ level of theory and vibrational entropy with ANI-2x⁴⁴ machine learning interatomic potential. As expected, at low temperatures, α has lower free energy. Due to higher entropy, the free energy of β decreases faster with increasing temperature, and β is a more stable polymorph at high temperatures. Free energies cross at $T = 136$ K, considerably lower than in experiments, but due to the very small angle at which free energies cross, considering approximations, this is a reasonable prediction.⁴⁵ Note that at laboratory conditions, Gibbs free energy is minimized, but for computational convenience, and since we have used experimental unit cells, Helmholtz free energy is used instead. Usually, kinetic barrier is associated with a polymorphic transition, even when the free energies of the two polymorphs are the same. For that reason, during heating, a phase transition will happen only at a higher temperature compared to one at which free energies cross each other. On the other hand, milling can overcome such a barrier, and phase transition can happen at the temperature at which free energies cross each other. This concept of different temperatures of phase transitions when heating and thermo-milling is indicated in ESI,† Fig. S13.

In summary, we measured the onset and completion temperatures of $\alpha \rightarrow \beta$ polymorphic transitions in 1-adamantyl-1-diamantyl ether. We determined that the transition temperature

is 31 °C lower under thermo-mechanochemical conditions than the corresponding DSC transition temperature.|| A combined experimental and computational analysis indicates that milling overcomes the kinetic barrier for the polymorph transition. Calculated Helmholtz free energies as a function of temperature for the two polymorphs confirmed their relative stabilities, in agreement with the experiments. Our findings show that thermo-mechanochemistry may open a pathway towards solid forms not available by conventional heating techniques and advance the fundamental understanding of polymorphic transitions of organic molecular crystals. Furthermore, the ability to manipulate polymorphic transition temperatures might have commercial consequences, for example, in patent claims.

J. A. and T. S. conceptualized the project and performed the experiments. J. A., M. Š., K. U., and T. S. supervised the project. M. Š. and K. U. acquired funding. I. L. performed DFT and machine learning interatomic potential calculations. M. E. assisted with DESY *in situ* monitoring. M. R. performed DSC experiments. Z. Š. solved the crystal structure of β . J. A. and T. S. wrote the original draft and all authors contributed to the final manuscript version.

Conflicts of interest

There are no conflicts to declare.

Acknowledgements

We thank Mr Tomislav Mrla for his help with thermo-mechanochemical setup. J. A. acknowledges the CERIC-ERIC Consortium for access to experimental facilities (proposal 20222189) and Dr Andraž Krajnc and Ms Marija Švegovec for CPMAS NMR data collection. T. S. and K. U. acknowledge DESY (Hamburg, Germany) for the provision of experimental facilities. Parts of this research were carried out at PETRA III, beamline P02.1. Beamtime was allocated for proposal I-20220019 EC. K. U., M. Š., and I. L. acknowledge the Croatian Science Foundation (grants IP-2020-02-4702, UIP-2017-05-9653, and UIP-2020-02-5675) for financial support.

Notes and references

§ Here, we define the onset and completion temperatures of polymorphic transitions under thermo-mechanochemical conditions as the temperatures of the first appearance of diffraction peaks corresponding to a different polymorph and the presence of a single polymorphic phase in the reaction mixture (by *in situ* synchrotron PXRD and temperature monitoring).

¶ LAG with *n*-pentane changes the starting free-flowing powder to flakes. This was visually observed by opening the milling jar.

|| The difference of 31 °C was calculated by using the lowest milling temperature of $\alpha \rightarrow \beta$ transition and the DSC peak temperature of $\alpha \rightarrow \beta$ transition by applying a 10 °C min⁻¹ heating rate. We acknowledge the fact that the transition temperature difference is dependent on a DSC heating rate.

1 J. Cruz-Cabeza, S. M. Reutzel-Edens and J. Bernstein, *Chem. Soc. Rev.*, 2015, **44**, 8619.



2 A. Nogueira, C. Castiglioni and R. Fausto, *Commun. Chem.*, 2020, **3**, 34.

3 H. Chunga and Y. Diao, *J. Mater. Chem. C*, 2016, **4**, 3915.

4 T. Stolar and K. Užarević, *CrystEngComm*, 2020, **22**, 4511.

5 P. Naumov, D. P. Karothu, E. Ahmed, L. Catalano, P. Commins, J. M. Halabi, M. B. Al-Handawi and L. Li, *J. Am. Chem. Soc.*, 2020, **142**, 13256.

6 K. Kawakami, *J. Pharm. Sci.*, 2007, **96**, 982.

7 J. Anwar and D. Zahn, *Adv. Drug Delivery Rev.*, 2017, **117**, 47.

8 S. L. James, C. J. Adams, C. Bolm, D. Braga, P. Collier, T. Friščić, F. Grepioni, K. D. M. Harris, G. Hyett, W. Jones, A. Krebs, J. Mack, L. Maini, A. G. Orpen, I. P. Parkin, W. C. Shearouse, J. W. Steed and D. C. Waddell, *Chem. Soc. Rev.*, 2012, **41**, 413.

9 T. Friščić, C. Mottillo and H. M. Titi, *Angew. Chem., Int. Ed.*, 2020, **59**, 1018.

10 A. A. L. Michalchuk, E. V. Boldyreva, A. M. Belenguer, F. Emmerling and V. V. Boldyrev, *Front. Chem.*, 2021, **9**, 685789.

11 K. Linberg, P. Szymoniak, A. Schonhals, F. Emmerling and A. Michalchuk, *Chem. – Eur. J.*, 2023, e202302150.

12 N. Shan, F. Toda and W. Jones, *Chem. Commun.*, 2002, 2372.

13 T. Friščić, A. V. Trask, W. Jones and W. D. S. Motherwell, *Angew. Chem., Int. Ed.*, 2006, **45**, 7546.

14 A. M. Belenguer, G. I. Lampronti, N. De Mitri, M. Driver, C. A. Hunter and J. K. M. Sanders, *J. Am. Chem. Soc.*, 2018, **140**, 17051.

15 T. Stolar, J. Alić, I. Lončarić, M. Etter, D. Jung, O. K. Farha, I. Đilović, E. Meštrović and K. Užarević, *CrystEngComm*, 2022, **24**, 6505.

16 T. Friščić, D. Reid, I. Halasz, R. Stein, R. Dinnebier and M. Duer, *Angew. Chem., Int. Ed.*, 2010, **49**, 712.

17 D. Hasa, E. Carlino and W. Jones, *Cryst. Growth Des.*, 2016, **16**, 1772.

18 L. S. Germann, M. Arhangelskis, M. Etter, R. E. Dinnebier and T. Friščić, *Chem. Sci.*, 2020, **11**, 10092.

19 K. Linberg, F. Emmerling and A. A. L. Michalchuk, *Cryst. Growth Des.*, 2023, **23**, 19.

20 A. A. L. Michalchuk, I. A. Tumanov and E. V. Boldyreva, *J. Mater. Sci.*, 2018, **53**, 13380.

21 K. Užarević, N. Ferdelji, T. Mrla, P. A. Julien, B. Halasz, T. Friščić and I. Halasz, *Chem. Sci.*, 2018, **9**, 2525.

22 K. Linberg, B. Röder, D. Al-Sabbagh, F. Emmerling and A. A. L. Michalchuk, *Faraday Discuss.*, 2023, **241**, 178.

23 T. Friščić, I. Halasz, P. J. Beldon, A. M. Belenguer, F. Adams, S. A. J. Kimber, V. Honkimäki and R. E. Dinnebier, *Nat. Chem.*, 2013, **5**, 66.

24 K. Užarević, I. Halasz and T. Friščić, *J. Phys. Chem. Lett.*, 2015, **6**, 4129.

25 A. A. L. Michalchuk and F. Emmerling, *Angew. Chem., Int. Ed.*, 2022, **61**, e202117270.

26 N. Cindro, M. Tireli, B. Karadeniz, T. Mrla and K. Užarević, *ACS Sustainable Chem. Eng.*, 2019, **7**, 16301.

27 V. Martinez, T. Stolar, B. Karadeniz, I. Brekalo and K. Užarević, *Nat. Rev. Chem.*, 2023, **7**, 51.

28 J. Alić, I. Biljan, Z. Štefanić and M. Šekutor, *Nanotechnology*, 2022, **33**, 355603.

29 H. Schwertfeger, A. A. Fokin and P. R. Schreiner, *Angew. Chem., Int. Ed.*, 2008, **47**, 1022.

30 M. A. Gunawan, J.-C. Hierso, D. Poinset, A. A. Fokin, N. A. Fokina, B. A. Tkachenko and P. R. Schreiner, *New J. Chem.*, 2014, **38**, 28.

31 W. L. Yang, J. D. Fabbri, T. M. Willey, J. R. I. Lee, J. E. Dahl, R. M. K. Carlson, P. R. Schreiner, A. A. Fokin, B. A. Tkachenko, N. A. Fokina, W. Meevasana, N. Mannella, K. Tanaka, X. J. Zhou, T. van Buuren, M. A. Kelly, Z. Hussain, N. A. Melosh and Z.-X. Shen, *Science*, 2007, **316**, 1460.

32 C. E. Nordman and D. L. Schmitkons, *Acta Cryst.*, 1965, **18**, 764.

33 P. D. Harvey, D. F. R. Gilson and I. S. Butler, *Can. J. Chem.*, 1987, **65**, 1757.

34 T. Salzillo, A. Girlando and A. Brillante, *J. Phys. Chem. C*, 2021, **125**, 7384.

35 E. O. R. Beake, M. G. Tucker, M. T. Dove and A. E. Phillips, *ChemPhysChem*, 2016, **18**, 459.

36 P. Negrier, M. Barrio, J. Ll. Tamarit and D. Mondieig, *J. Phys. Chem. B*, 2014, **118**, 9595.

37 P. Negrier, M. Barrio, M. Romanini, J. Ll. Tamarit, D. Mondieig, A. I. Krivchikov, L. Kepinski, A. Jezowski and D. Szewczyk, *Cryst. Growth Des.*, 2014, **14**, 2626.

38 P. Negrier, B. B. Hassine, M. Barrio, M. Romanini, D. Mondieig and J. Ll. Tamarit, *CrystEngComm*, 2020, **22**, 1230.

39 A. Salvatori, P. Negrier, S. Massip, A. Muñoz-Duque, P. Lloveras, M. Barrio and J.-L. Tamarit, *CrystEngComm*, 2022, **24**, 3692.

40 J. Alić, T. Stolar, Z. Štefanić, K. Užarević and M. Šekutor, *ACS Sustainable Chem. Eng.*, 2023, **11**, 617.

41 J. Alić, R. Messner, M. Alešković, F. Küstner, M. Rubčić, F. Lackner, W. E. Ernst and M. Šekutor, *Phys. Chem. Chem. Phys.*, 2023, **25**, 11951.

42 J. P. Perdew, K. Burke and M. Ernzerhof, *Phys. Rev. Lett.*, 1996, **77**, 3865.

43 A. Ambrosetti, A. M. Reilly, R. A. DiStasio Jr and A. Tkachenko, *J. Chem. Phys.*, 2014, **140**, 18A508.

44 C. Devereux, J. S. Smith, K. K. Huddleston, K. Barros, R. Zubatyuk, O. Isayev and A. E. Roitberg, *J. Chem. Theory Comput.*, 2020, **16**, 4192.

45 D. Firaha, Y. M. Liu, J. van de Streek, K. Sasikumar, H. Dietrich, J. Helfferich, L. Aerts, D. E. Braun, A. Broo, A. G. DiPasquale, A. Y. Lee, S. Le Meur, S. O. Nilsson Lill, W. J. Lunsmann, A. Mattei, P. Muglia, O. D. Putra, M. Raoui, S. M. Reutzel-Edens, S. Rome, A. Y. Sheikh, A. Tkatchenko, G. R. Woollam and M. A. Neumann, *Nature*, 2023, **623**, 324.

